Edinburgh Research Explorer

Multiple time grids in operational optimisation of energy systems with short- and long-term thermal energy storage

Multiple time grids in operational optimisation of energy systems with short- and long-term thermal energy storage

Renaldi Renaldi[a,∗], Daniel Friedrich[a]

[a]*Institute for Energy Systems, School of Engineering, University of Edinburgh, Colin Maclaurin Road, Edinburgh EH9 3DW, UK*

Abstract

As a vital part of future low carbon energy systems, storage technologies need to be included in the overall optimisation of energy systems. However, this comes with a price of increasing complexity and computational cost. The increase in complexity can be limited by using simplified time series formulations in the optimisation process, e.g. typical days or multiple time grids. This in turn will affect the computational cost and quality of the optimisation results. The trade-off between these two aspects has to be quantified in order to appropriately use the simplification method. This paper investigates the implementation of the multiple time grids approach in the optimisation of a solar district heating system with short- and long-term thermal energy storage. The multiple time grids can improve the optimisation computational time by over an order of magnitude. Nevertheless, this is not a general rule since it is shown that there is a possibility for the computational time to increase with time step size. Furthermore, the benefits of multiple time grids become more evident in optimisation with a longer time horizon, reaching almost two order of magnitude improvement in computational time for the case with 6 years time horizon and 5% MIP gap.

Keywords: thermal energy storage, seasonal storage, optimisation, district heating, mixed integer linear programming

1. Introduction

Energy storage has been acknowledged as a vital technology required to achieve a low carbon energy system [1]. It has wide variety covering different

---

∗Corresponding author.
Email addresses: `r.renaldi@ed.ac.uk` (Renaldi Renaldi), `d.friedrich@ed.ac.uk` (Daniel Friedrich)

Nomenclature

A	area, m^2		c	heat capacity, kJ/kgK
BOI	boiler		ch	charge
C	cost, \$/kWh		dch	discharge
$DLSC$	Drake Landing Solar Community			
			el	electricity
G	global horizontal irradiance, kJ/m^2		gas	natural gas
HD	heating demand		n	index of time point set
HX	heat exchanger		opr	operational
LTS	long-term storage			
MU	multiple uniform		s	soil
MNU	multiple non-uniform		sto	store
P	electrical power, kW		t	time step
Q	thermal energy, kWh		w	water
$\dot{Q}$	thermal power, kW			
SU	single uniform		ϵ	time point
SNU	single non-uniform		η	efficiency, -
SCO	solar collector		δ	time step size, h
SOC	state-of-charge			
STS	short-term storage		ρ_w	density, kg/m^3
T	temperature, K		ϕ	standing losses, %
V	volume, m^3		ψ	state of LTS

form of energy (electrical, thermal, mechanical, and chemical), various energy-to-power ratio, and the potential of multitude value contributions to the energy system. For instance, storage can increase the utilisation of renewable energy by overcoming the supply-demand mismatch inherent in wind and solar energy [2]. Furthermore, if transport and heat are powered by low carbon electricity, storage can improve demand side management and providing ancillary services for energy suppliers [3, 4].

These and other benefits of energy storage can be ensured and increased further by optimising the design and operation of the overall energy systems. For example, the size and charge/discharge behaviour of a storage equipment will influence the trade-off between the capital and operational costs of the overall system. This is typically included in the optimisation study of an energy

2

system, for example in the case of building energy systems [5], microgrids [6], district heating networks [7], and urban energy systems [8].

However, the presence of storage can significantly increase the optimisation problem complexity due to (i) the coupling of decisions between time steps, i.e. the stored energy at time step t will influence the operational decisions at $t + 1$; (ii) the additional decision variables for every time step, i.e. decision to charge, discharge or store the energy; and (iii) the time resolution required to appropriately model the storage behaviour [9].

This increasing complexity of energy systems optimisation can be contained by various reduction techniques on the two main modelling aspects of the optimisation: the time series and the equipment modelling. The former refers to how the time horizon and time steps are defined in the optimisation process, while the latter refers to the accuracy of the equipment model. Complexity reduction by modifying the equipment model is relatively straightforward to examine since it is known that a more detailed and accurate model will typically have higher computational cost than a simplified one. Studies on the trade-off between modelling accuracy and computational time of specific equipment have been reported in the literature, e.g. air source heat pump [10], combined heat and power [11], and hot water tank storage [12]. On the other hand, reducing the problem complexity by using different time series modelling formulation has been less well studied, especially in problems with integrated storage equipment.

In most optimisation studies that include storage equipment, the time series modelling simplification is generally performed using typical period assumption with single time grid, e.g. one typical day with hourly time step as a representative of a whole season. Despite its usefulness in systems with one type of storage technology, this approach is not able to fully capture the behaviour of systems with different storage temporal characteristics. One prominent example of such systems is a solar thermal heating system with short- and long-term thermal energy storage. The short-term storage operates on a daily or weekly cycle, while the long-term storage operates on a monthly or even seasonal cycle. Studies on such systems have been reported in the literature and mostly use single time grid in simulating and optimising the system [13, 14, 15].

An alternative to the typical period approach is the use of multiple time grids in the optimisation model. In the multiple time grids method, every equipment can have its own time grid which corresponds to its characteristics. The concept of multiple time grids has been explored in the field of process systems engineering (e.g. [16, 17, 18] and electric power system (e.g [19, 20, 21]). Nevertheless, its implementation on energy systems with different types of storage is less well studied, particularly for systems with seasonal storage.

The present work aims to fill this gap by investigating the implementation of the multiple time grids formulation in the optimisation of energy systems with multiple storage technologies. The considered system is a solar district heating installation with short- and long-term thermal energy storage. Different time grids formulations were then implemented within the mixed-integer linear programming (MILP) optimisation. The results between optimisation run were compared in terms of their relative error and computational cost. The trade-off

3

between these two aspects are central in the contributions of this work to the body of knowledge.

In the following section, a brief overview of time series modelling in energy systems optimisation, including the multiple time grids approach, is presented first. Details on the implementation of the multiple time grids approach on the case study are then given, along with the discussion on the optimisation results and comparison between time grids formulations.

2. Time series modelling

The representation of time in an operational optimisation problem has been widely investigated over the past decades, particularly in the field of process systems engineering where various continuous- and discrete-time representations have been proposed and implemented [16]. In energy systems optimisation, discrete-time representation is typically used over continuous-time because of the nature of the energy demand profile.

As briefly mentioned in the previous section, the most common way to reduce the problem size in energy systems optimisation is by using the typical periods approach. The main assumption of this approach is that a certain time horizon, typically a year, can be represented by a set of periods, e.g. days, weeks or months. An example is using one typical day for each season in a year, thus reducing the number of hourly time steps from 8760 to 96 hours.

Apart from empirical selection of typical periods, different methods to systematically determine typical periods have been proposed in the literature. Mavrotas et al. investigated the effect of data compression on the model accuracy [22]. They reduced the demand data by performing systematic grouping of months to seasons and hours to intraday periods. Ortiga et al. proposed a graphical method to select typical days representation from hourly energy demand data [23]. The issue of subjectivity inherent in a graphical method has been minimised by the proposed systematic approach of Dominguez-Munoz et al. [24]. In this method, typical days are selected by applying a k-medoid clustering algorithm to the whole year demand data. Fazlollahi et al. developed a systematic approach which selects typical days by using the k-means partitioning clustering algorithm and optimising the results by means of ϵ-constraints technique [25]. They also reported the accuracy of the optimisation results using typical days relative to the one using full time steps. It should be noted that storage equipment were not included in the aforementioned studies on typical days determination methods.

In the second part of their study, Fazlollahi et al. implemented the systematic typical days selection method on a case study with daily thermal energy storage [26]. The inclusion of daily storage was also considered by Soderman and Patterson in their optimisation with two typical periods for each season [27]. As in other reported optimisation works which consider storage equipment, these two studies also implemented a cyclic constraint for the storage equipment, i.e. the state-of-charge of the storage in the first step of a period equals the state-of-charge in the last step of the previous period.

4

Besides daily storage, several studies on optimisation of systems with seasonal storage have also been reported. Tveit et al. empirically selected 13 periods per year in the optimisation of district heating networks with seasonal thermal energy storage [13]. They did not assume the cyclic behaviour of the seasonal storage; therefore, the first and last period of the resulting storage profile are less realistic than the other periods. Samsatli and Samsatli used a non-uniform hierarchical time discretisation in order to reduce the problem size of optimising a hydrogen network with integrated storage [28]. In the study, the behaviour of storage over different time periods were defined by prescribing constraints which linked its inventory between typical days, weeks and seasons for an entire year. However, the assumption that the system is periodic has to be taken in order to implement this method.

Although the typical periods method is able to reduce the complexity of problems with one type of storage, its application to systems with multiple storages which operate on different temporal scales still produces a relatively large problems due to the usage of two detailed time scales [29]. Further complication might arise if these storages are connected to each other, as it is normally the case in solar district heating systems. A potential technique to overcome these problems is the multiple time grids method.

2.1. Multiple time grids

The main idea in the multiple time grids method is to formulate an optimisation model that use different time grids for each equipment, resources, and materials [30, 31, 32]. It has been proposed as a way to reduce the number of time steps in scheduling problems [16]. Although it is mainly developed in continuous-time representation, recent studies have shown that it is also applicable in discrete-time representation [17, 18].

As illustrated in Fig. 1, time grids in discrete time optimisation can be categorised into four types: single-uniform (SU), single-non-uniform (SNU), multiple-uniform (MU), and multiple-non-uniform (MNU) time grids [17]. In single time grid, all equipment is modelled using one time grid, while in multiple time grid, every equipment can have its own time grid. Furthermore, the uniformity aspect of the grid corresponds to the step size(s) of the time grid, e.g. in Fig. 1.b, all equipment have two time step sizes: 1 and 4h. Currently, a SU time grid is the one typically used in energy systems optimisation, with the grid size determined by the energy demand profile and operating characteristics of the considered equipment. Although an hourly time step is generally implemented, various step sizes have also been used in the literature. For example, Rieder et al. considered a 4 h time interval in their optimisation study due to a compromise between computational cost and the ability to capture the behaviour of the considered storage technology [7], while Tveit et al. captured the behaviour of seasonal storage with 13 periods per year [13].

In increasingly distributed and multi-vectors energy systems, equipment and demand may have very different temporal characteristics which are suitable for the implementation of the multiple time grids method. For example, solar district heating systems usually use both short- and long-term thermal energy
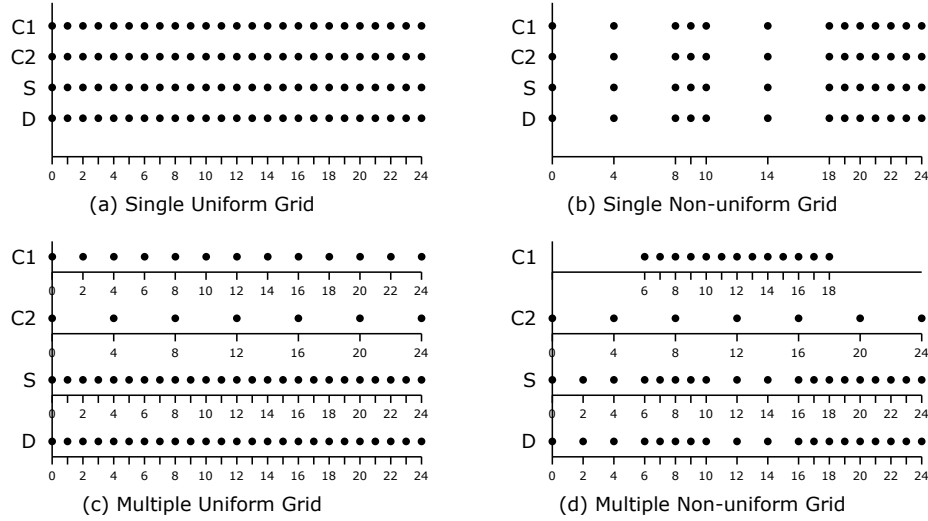
5

Figure 1: Types of time grids. Conversion equipment (C1, C2), storage equipment (S), and demand (D) time grids over 24 hours period are shown for illustrative purposes.

storage in order to increase the solar fraction [33]. The short-term storage typically operates on a daily or weekly cycle, while the long-term one operates on monthly or even seasonal cycle. This makes such system an interesting case study for the implementation of the multiple time grids method.

3. Implementation of multiple time grids

The schematic of the overall work flow in this study is illustrated in Fig. 2. Central to the work is the operational optimisation of the energy system, which was performed with different time grids formulations. Inputs to the operational optimisation include modelled heating demand profile, weather data, and equipment data. The optimisation results of different time grids formulations were then compared in terms of their computational time and relative accuracy. Furthermore, the influence of equipment characteristic on grid size selection and the multi-year optimisation with different time grids were also investigated.

The considered energy system in this study is Drake Landing Solar Community (DLSC) energy system, a solar district heating installation in Okotoks, Canada [34]. The system consists of solar thermal collectors, short-term storage, long-term storage and back-up boilers. It covers the space heating demand of 52 connected houses. Figure 3 illustrates the schematic of DLSC.

The solar collectors in DLSC are flat-plate glazed collectors with a total area of 2293 m^2. Two horizontal hot water tanks with a combined capacity of 240 m^3 act as the short-term thermal energy storage (STS) in DLSC. The STS can be charged by energy from the solar collectors and/or from the long-term storage. The long-term thermal storage (LTS) in DLSC is a borehole thermal
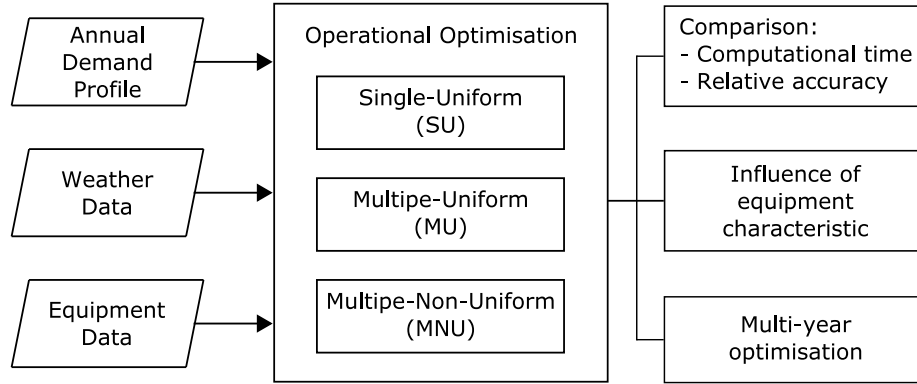
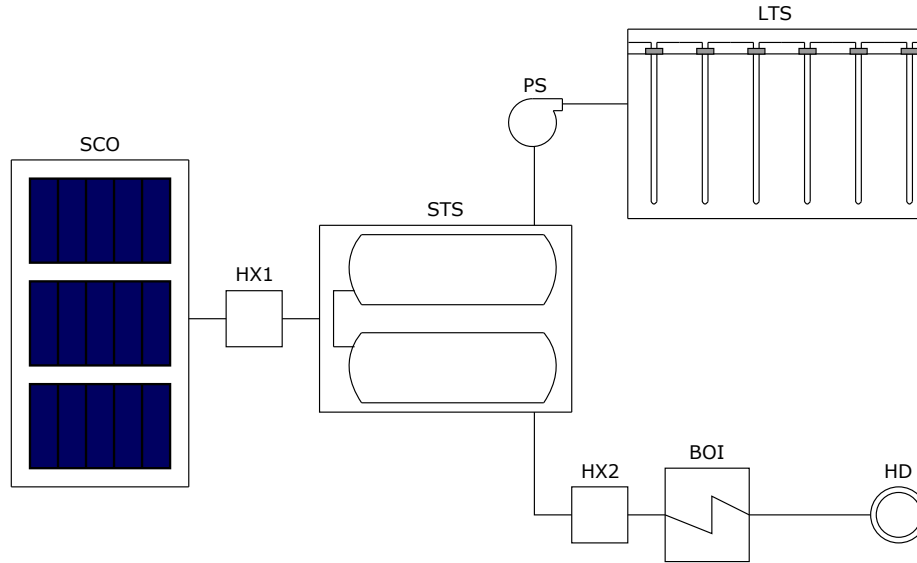Figure 2: Overall work flow of the optimisation study.

Figure 3: Schematic of the Drake Landing Solar Community. Main equipment are solar collectors (SCO), short-term thermal energy storage (STS), long-term thermal energy storage (LTS), and back-up gas boilers (BOI). They operate to supply the heat demand (HD) of the connected houses. Two heat exchangers (HX1, HX2) and one pump between the two storages (PS) were also modelled in the problem formulation.

energy storage which consists of 144 boreholes of 35 m depth. In recent years, DLSC has been subjected to several studies related to its operational control [35], storage design [36, 37], and performance on different locations [38].

3.1. Problem statement

In the current study, operational optimisation of DLSC was performed using mixed integer linear programming (MILP) formulation. The superstructure and

equipment size of the energy system were given as inputs to the optimisation problem, along with demand and weather data. The optimisation problem was a deterministic one; thus, perfect knowledge of future demand and weather conditions were assumed. The optimisation objective was to determine the operational profile over a time horizon that minimise the total operational cost, as shown in Eq. 1.

$$\min C_{opr} = \min \sum_{t_{start}}^{t_{end}} \left(\dot{Q}_{boi}(t) \cdot \Delta t \cdot C_{gas} + P_{pump}(t) \cdot \Delta t \cdot C_{el} \right) \quad (1)$$

The first term on the right hand side of Eq. 1 represents the fuel cost of the back-up boilers, while the second term corresponds to the electricity cost due to pump operations. In reality, there are five pumps in DLSC, one for every loop and with four of them having a parallel back-up [39]. Only one pump was modelled in this study because the focus of the study is on the effect of the LTS time grids rather than finding the detailed optimised profile of all the pumps. Furthermore, it has been shown that managing the interaction between STS and LTS is very important in the effort to increase the share of renewable energy in the system [40].

3.2. Implemented time grids

Velez and Maravelias proposed a set of algorithms to generate non-uniform time grids for short-term scheduling of chemical processes [17, 18]. Essentially, the algorithms examined the temporal characteristics of the units, tasks, and materials involved in the scheduled processes, and formulated multiple grids according to a set of requirements which should not be violated. In energy systems, these correspond to the characteristics of the main equipment and the energy demand.

In this study, the multiple time grids were generated based on empirical examination of the energy system. Time point set and time step size of equipment e is denoted by ϵ^e and δ^e, respectively. These are illustrated in Fig. 4 for an exemplary MU time grids of DLSC with $\delta^{sco} = \delta^{sts} = \delta^{hd} = 2$ h, and $\delta^{lts} = 6$ h. Since the difference in temporal characteristics of STS and LTS is the focus in this study, different δ^{lts} were tested in the optimisation run, ranging from 1 up to 24 h. Table 1 lists all the tested time grid step sizes in this study.

3.3. Mathematical model

The equipment modelling approach followed in this study is based on the first law of thermodynamics; hence, it implements only the energy balance and does not include the dynamics of, for example, mass flow rate and temperature in the system. Although it has been shown that this type of formulation may lead to less accurate representation of real systems (e.g. in [12] for the case of thermal energy storage), it is necessary to limit the equipment modelling
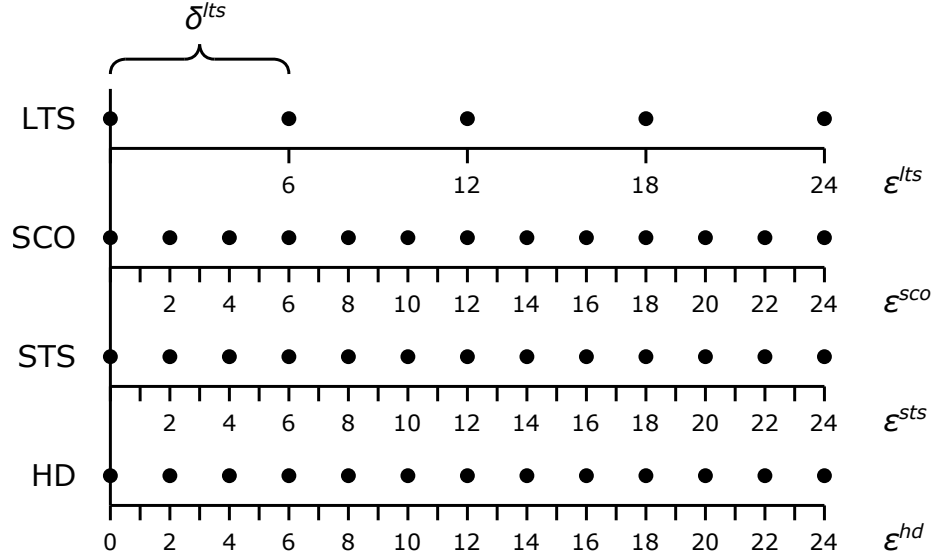
Figure 4: Example of multiple-uniform grids of DLSC with $\delta^{sco} = \delta^{sts} = \delta^{hd} = 2$ h, and δ^{lts} = 6 h.

complexity since the main focus of this study is not on the absolute accuracy, but on the effects of different time grid formulations on the optimisation results.

Optimisation variables are denoted in bold italic typeface, while parameters are in regular italic typeface. Furthermore, in order to improve the readability of equations, all equipment abbreviations inside equations are shown in lowercase, e.g. STS = sts. Parameters used in the optimisation run, along with their reference, are listed in Table 2.

3.3.1. Solar collector

The efficiency of the solar collector was assumed to be constant at $\eta^{sco} = 50\%$. This value was taken from observation of the collector efficiency graph

Table 1: Tested time grid step sizes

Time grids	SU	MU	MNU
δ^{sco}	$\{1, 2, 4, 6, 12, 24\}$	$\{1\}$	(non-uniform)
δ^{sts}	$\{1, 2, 4, 6, 12, 24\}$	$\{1\}$	$\{1\}$
δ^{lts}	$\{1, 2, 4, 6, 12, 24\}$	$\{1, 2, 4, 6, 12, 24\}$	$\{1, 2, 4, 6, 12, 24\}$
δ^{hd}	$\{1, 2, 4, 6, 12, 24\}$	$\{1\}$	$\{1\}$

in [34]. The constant efficiency approach in modelling the solar collector was followed because the flow inlet temperature was not modelled. Assuming this temperature as a constant would result in a very low efficiency figure at times when the ambient temperature is low, e.g. during winter period. Thus, the absorbed incident solar irradiation Q_t^{sco} was treated as a parameter and calculated with Eq. 2.

$$Q_t^{sco} = \eta^{sco} \cdot G_t \cdot A^{sco} \tag{2}$$

3.3.2. Short-term storage

The short-term storage was modelled with Eq. (3) - (9), which are widely used in modelling storage equipment in linear programming optimisation of energy systems.

The maximum stored energy Q_{max}^{sts} is calculated by Eq. (3) with the assumption of $\Delta T^{sts} = 50$ K. This yields a maximum stored energy of 50.4 GJ. The stored energy for every time step is calculated with Eq. (4). Furthermore, Eq. (5) - (7) represent constraints for maximum stored energy, charge rate and discharge rate, respectively. It should be noted that for cases with non-hourly time grids, the charge and discharge power are the average for the given time step. Furthermore, the STS state-of-charge is calculated by Eq. (8) and the cyclic behaviour of STS is defined by the constraint in Eq. (9).

$$Q_{max}^{sts} = \frac{V^{sts} \cdot \rho_w \cdot c_w \cdot \Delta T^{sts}}{3600} \tag{3}$$

$$\boldsymbol{Q}_{sto,t}^{sts} = (1 - \phi^{sts})^{\delta^{sts}} \cdot \boldsymbol{Q}_{sto,t-1}^{sts}$$
$$+ \left(\dot{\boldsymbol{Q}}_{ch,t}^{sts} - \dot{\boldsymbol{Q}}_{dch,t}^{sts} \right) \cdot \delta^{sts} \tag{4}$$

$$0 \leq \boldsymbol{Q}_{sto,t}^{sts} \leq Q_{max}^{sts} \tag{5}$$

$$0 \leq \dot{\boldsymbol{Q}}_{ch,t}^{sts} \leq \dot{Q}_{ch,max}^{sts} \tag{6}$$

$$0 \leq \dot{\boldsymbol{Q}}_{dch,t}^{sts} \leq \dot{Q}_{dch,max}^{sts} \tag{7}$$

$$\boldsymbol{SOC}_t^{sts} = \boldsymbol{Q}_{sto,t}^{sts} / Q_{max}^{sts} \tag{8}$$

$$\boldsymbol{SOC}_{t=0}^{sts} = \boldsymbol{SOC}_{t=t_{end}}^{sts} \tag{9}$$

10

3.3.3. Long-term storage

Similar to the STS, the LTS was modelled using the capacity model which assumes a fully distributed temperature inside the storage medium. However, unlike the STS, the LTS cannot be charged and discharged at the same time. This limitation is formulated as constraints in Eq. (13) - (15), in which the binary variable ψ corresponds to the charging ($\psi_{ch} = 1, \psi_{dch} = 0$), discharging ($\psi_{ch} = 0, \psi_{dch} = 1$) or store ($\psi_{ch} = \psi_{dch} = 0$) status of the LTS.

$$Q_{lts}^{max} = \frac{V_{lts} \cdot \rho_s \cdot c_s \cdot \Delta T_{lts}}{3600} \tag{10}$$

$$\boldsymbol{Q}_{sto,t}^{lts} = (1 - \phi_{lts})^{\delta^{lts}} \cdot \boldsymbol{Q}_{sto,t-1}^{lts}$$
$$+ \left(\dot{\boldsymbol{Q}}_{ch,t}^{lts} - \dot{\boldsymbol{Q}}_{dch,t}^{lts} \right) \cdot \delta^{lts} \tag{11}$$

$$0 \leq \boldsymbol{Q}_{sto,t}^{lts} \leq Q_{max}^{lts} \tag{12}$$

$$0 \leq \dot{\boldsymbol{Q}}_{ch,t}^{lts} \leq \boldsymbol{\psi}_{ch,t}^{lts} \cdot \dot{Q}_{ch,max}^{lts} \tag{13}$$

$$0 \leq \dot{\boldsymbol{Q}}_{dch,t}^{lts} \leq \boldsymbol{\psi}_{dch,t}^{lts} \cdot \dot{Q}_{dch,max}^{lts} \tag{14}$$

$$\boldsymbol{\psi}_{ch,t}^{lts} + \boldsymbol{\psi}_{dch,t}^{lts} \leq 1 \tag{15}$$

$$\boldsymbol{SOC}_t^{lts} = \boldsymbol{Q}_{sto,t}^{lts} / Q_{max}^{lts} \tag{16}$$

$$\boldsymbol{SOC}_{t=0}^{lts} = \boldsymbol{SOC}_{t=t_{end}}^{lts} \tag{17}$$

The implementation of the multiple time grids method in this study is particularly focused on the LTS time grid. It should be emphasised that the status of LTS is fixed for every time step, regardless of the time step size. For example, if $\boldsymbol{\psi}_{ch,t}^{lts} = 1$ in MU case with $\delta^{lts} = 6$ h, it means that the LTS is constantly charging for 6 h between $\epsilon_n^{lts} = t$ and ϵ_{n+1}^{lts}.

3.3.4. Heat exchangers

The energy balance between supply and demand was formulated as the constraints describing the two main heat exchangers in the system. The first heat exchanger (HX1) transfers solar energy from the collector to the short term storage (Eq. (18) - (19)), while the second heat exchanger (HX2) satisfies the heating demand by the energy from STS discharge and the backup boilers (Eq. (20)).

$$\dot{\boldsymbol{Q}}_t^{sco-hx1} \leq \dot{Q}_t^{sco} \tag{18}$$

$$\dot{Q}_t^{sco-hx1} = \begin{cases} \dot{\boldsymbol{Q}}_{ch,t}^{sts} - \dot{\boldsymbol{Q}}_{dch,t}^{lts} & \text{if } t \text{ in } \epsilon^{lts} \\ \dot{\boldsymbol{Q}}_{ch,t}^{sts} - \dot{\boldsymbol{Q}}_{dch,t=\epsilon_{n-1}^{lts}}^{lts} & \text{otherwise} \end{cases} \tag{19}$$

$$\dot{Q}_t^{sts-hx2} = \begin{cases} \dot{\boldsymbol{Q}}_{dch,t}^{sts} - \dot{\boldsymbol{Q}}_{ch,t}^{lts} & \text{if } t \text{ in } \epsilon^{lts} \\ \dot{\boldsymbol{Q}}_{dch,t}^{sts} - \dot{\boldsymbol{Q}}_{ch,t=\epsilon_{n-1}^{lts}}^{lts} & \text{otherwise} \end{cases} \tag{20}$$

3.3.5. Heat demand and weather data

The heat demand in every time step is fulfilled by the solar energy that transferred through HX2 and the additional energy from the back-up boiler (Eq. (21)).

$$\dot{Q}_t^{hd} = \dot{\boldsymbol{Q}}_t^{sts-hx2} + \dot{\boldsymbol{Q}}_t^{boi} \tag{21}$$

The heating demand (HD) profile of the 52 houses was derived synthetically based on annual energy consumption, ambient temperature and assumed occupancy profiles, a similar modelling approach has been used in [44]. Ambient temperature and solar irradiation data were gathered from publicly available data [45, 46]. Two time horizons were selected for this study: one year and multi-year horizon. The selected timeline was from July 2012 to June 2013 for one year optimisation and July 2007 to June 2013 for multi-year optimisation. Hourly demand and weather data used in this study are available in the Supplementary Information. Demand is given in power unit (kW), while solar irradiation is in energy per unit area (kJ/m^2). Furthermore, in the implementation of time grids other than 1 hour, the energy demand and solar irradiation were averaged over the respective time steps.

3.3.6. DLSC control implementation

An optimisation model with the DLSC control rules was also developed and solved accordingly. This particular model serves as a comparison to the regular optimisation model, in which the solver tries to find the optimal control rather than using a pre-determined rule.

The implemented rules correspond to the control of interaction between STS and LTS during the winter period, as explained in [40]. The control rules determine when the LTS should start charging and discharging during the winter by comparing the STS state-of-charge to a pre-determined required state-of-charge. The latter depends on the set-point temperature of the district loop. Further details on the control rule can be found in [40].

The winter mode control rules were implemented in the optimisation model as two additional constraints (Eq. (22) and (23)) which were only applied during the winter months (Jan-Apr and Sep-Dec, inclusive). $SOC_{req,t}^{sts}$ is the required state-of-charge at time t and its value is given as a parameter (Appendix A).

$$\boldsymbol{SOC}_t^{sts} - SOC_{req,t}^{sts} \leq 0.75 \cdot \boldsymbol{\psi}_{ch,t}^{lts} \tag{22}$$
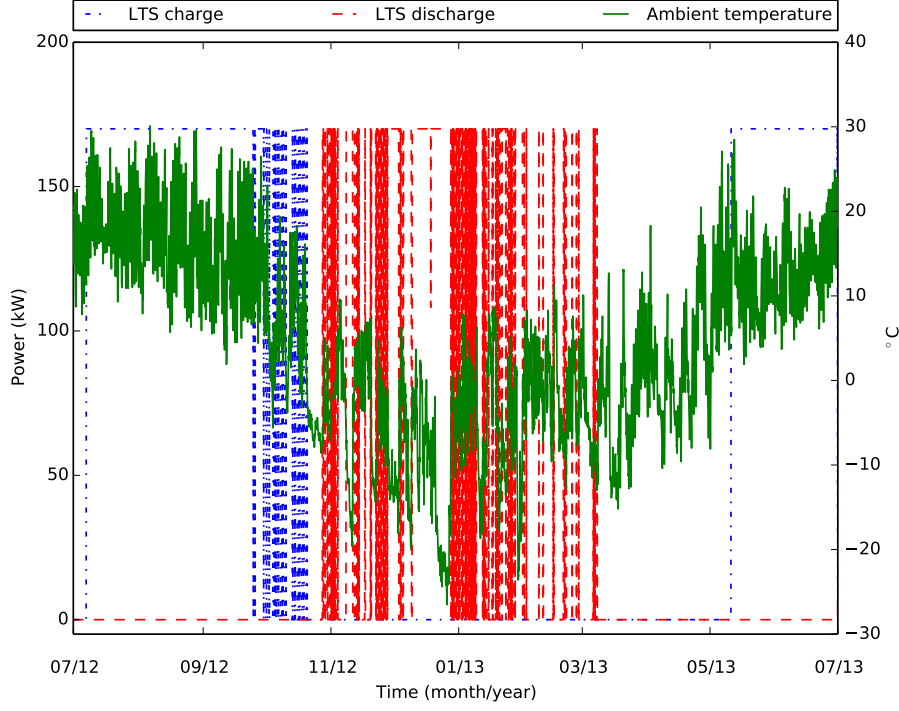
Figure 5: LTS charge/discharge profile for the reference case.

$$\boldsymbol{SOC}_t^{sts} - SOC_{req,t}^{sts} \geq -1 \cdot \boldsymbol{\psi}_{dch,t}^{lts} \qquad (23)$$

3.4. Modelling tools

The optimisation problem was formulated in Pyomo 4.0 [47] and solved with CPLEX 12.6.2 [48] on a Windows computer with a 3.4GHz i7 Intel processor and 16 GB of RAM. The time limit for every optimisation run is 3600 s. Computational times are defined as the time used by CPLEX to solve the optimisation problem and quoted as the wall time. The reported optimality gap refers to the relative tolerance between the best objective and the objective of the best node remaining, as defined by CPLEX.

4. Results and discussion

4.1. Reference case

In order to make a comparison between different time grid implementations, the single-uniform grid with 1h time step and 1% optimality gap was selected as the reference case. Its computational results are summarised in Table 3.

13

Furthermore, the resulting operational profiles of the LTS in the reference case are shown in Fig. 5. The charge and discharge profile are similar to the expected profile of a seasonal storage, i.e. charging in the summer and discharging in the winter. However, unlike the measured profile reported in [39], the optimised profile has a gap between mid-March and mid-May. This is because in the optimisation case, the solver has to look over the prescribed time horizon in order to produce the optimal profile. It is necessary to solve the optimisation simultaneously over the whole time horizon since the presence of storage has coupled the decisions between different time steps. In other words, the solver has full knowledge of the future; thus, it knows exactly when the charging is sufficient for the period ahead, avoiding unnecessary charging which may worsen the objective value.

4.2. Comparison between time grids: computational times and relative accuracy

Annual operation optimisations of DLSC were performed using single-uniform and multiple-uniform time grids with 1% and 5% optimality gap. The two optimality gap values were selected in order to illustrate the influence of the prescribed value on computational time and relative accuracy of the results.

Results of single-uniform cases are shown in Fig. 6. As expected, the computational time follows a decreasing trend as the grid size increases (Fig. 6(a)). This corresponds to the lower number of optimisation variables as the time grid becomes coarser. However, the decrease in computational time comes with the cost of increasing relative error of the objective value, as illustrated in Fig. 6(b). It should be noted that the error was calculated relative to the objective value of the reference case. Thus, Fig. 6(b) shows the relative error for optimisation run with different time step size. The increase in relative error is caused by the averaging of the demand profile which eliminates inherent peaks. In addition to an increase in relative error, it will also affect the equipment sizing if design optimisation is performed, e.g. undersized equipment due to missing peak demand. This observation is in line with the study on the effects of temporal precision in optimisation of residential cogeneration systems [49, 50]

In order to avoid the shortcomings of using a coarse single-uniform grid, the multiple-uniform grids approach was tested on the same optimisation problem. In measuring the computational time, the optimisation run with a LTS step size and optimality gap combination was repeated five times. The resulting average computational times and relative error are illustrated in Fig. 7. Overall, the computational time decreases as the LTS time step size increases from 1 to 24 h. However, unlike the single-uniform case, the computational time is not always decreasing with time step size. In this case, the computational time decreases by one order of magnitude as the LTS step size increases up to 2 h and 6 h for the 1% and 5% MIP gap case, respectively (Fig. 7(a)). Beyond these step sizes, the computational time has an increasing trend in both cases. This is significantly different than in single-uniform cases and can be explained by examining the operational characteristic of the LTS in the system.

The LTS serves as a large storage option to store excess solar energy during the summer and discharge them to the STS during the winter. Thus, as LTS
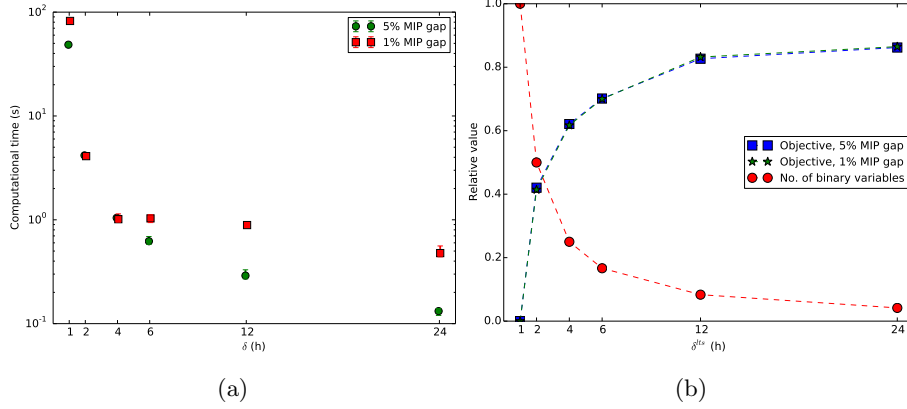
Figure 6: Results for single-uniform cases: (a) Computational time, and (b) Relative error of the objective function and number of binary variables for different time step size. Note that there is a significant overlap between the two objective function relative error curves. The dashed lines are shown as a guide to illustrate the trend.

charge/discharge behaviour is restricted to larger number of hours with increasing δ^{lts}, it becomes more difficult for the solver to find an optimal profile, since it means that a larger amount of energy must be available/unavailable within the STS. This illustrates that although the number of variables is reduced due to the use of coarser δ^{lts}, the problem can still become harder to solve. This observation is in line with a previous study which noted that the multiple grids model can have a worse solution time than the single uniform model [17].

Furthermore, despite the absence of consistent decreasing trend in the computational time, the increasing LTS step size has a relatively small effect on the objective value, as shown in Fig. 7(b). This feature makes the implementation of multiple-uniform grid a promising alternative in limiting the increase in computational cost due to time series modelling. Together with the results on computational time, a multiple-uniform approach with $\delta^{lts} = 6$ h and 5% MIP gap is the best combination for this case study.

In an attempt to further lower the computational time, a multiple-non-uniform (MNU) time grids was implemented in the case study. The non-uniformity of the grids stemmed from the SCO time grid which was prescribed to be only available during daytime; thus, reducing the number of variables even further. Nevertheless, the computational time and relative objective value for this case are practically the same with the multiple-uniform one. This is because the solar irradiation acted as a parameter in the formulation and the collected solar energy variable (Q^{sco}) was defined as a simple multiplication between irradiation and collector efficiency (Eq. 2). Therefore, a reduction in the number of this variable by removing the zero-valued due to unavailable solar irradiation has little impact on computational time. Furthermore, the pre-solve step employed by the solver may also contribute to the negligible impact of SCO time grid reduction. It should be noted that MNU time grids may have more
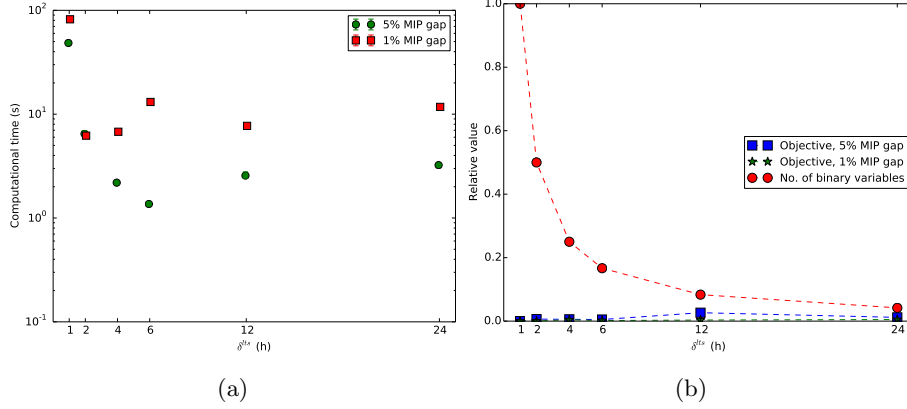
15

Figure 7: Results for multiple-uniform cases: (a) Computational time, and (b) Relative error of the objective function and number of binary variables for different LTS time step size. Note that there is a significant overlap between the two objective function relative error curves. The dashed lines are shown as a guide to illustrate the trend.

impacts in more complex models, for example in multi-vector energy system with various demand profiles.

From comparison between time grid implementations, it is clear that increasing the time step size in SU model can significantly affect the objective value, while this is not the case in the implemented MU model. However, the computational time reduction in the MU model is not always guaranteed by increasing the equipment time step size, in this case the LTS (δ^{lts}). For the modelled system, the computational time reaches a minimum before it starts an increasing trend with δ^{lts}, indicating an optimal δ^{lts} for a given system.

4.3. Grid size and equipment characteristics

In order to evaluate whether the optimal time grid size of a storage equipment depends on its characteristics, MU optimisation run with varying storage parameters were performed. One relevant characteristic is the storage thermal power (maximum charge/discharge rate). The MU optimisation run was performed using different LTS power and the resulting computational time graphs are shown in Fig 8.

The overall trend shows that as the LTS power grows, the use of large δ^{lts} becomes less beneficial due to increasing computational time. The case of 340 kW (Gap=1%) even failed to reached optimality within the prescribed time limit when 12 h time step is used. Moreover, apart from the case of 340 kW (Gap=1%), the test cases show an improvement in computational times as δ^{lts} is increased from 1 to 2 h. In the 340 kW (Gap=1%) case, the exception from this trend is relatively small compared to the drop of computational time in other cases.

Since the LTS operation is highly coupled to the STS, MU optimisation with different STS sizes were also performed in order to evaluate the possible effects.
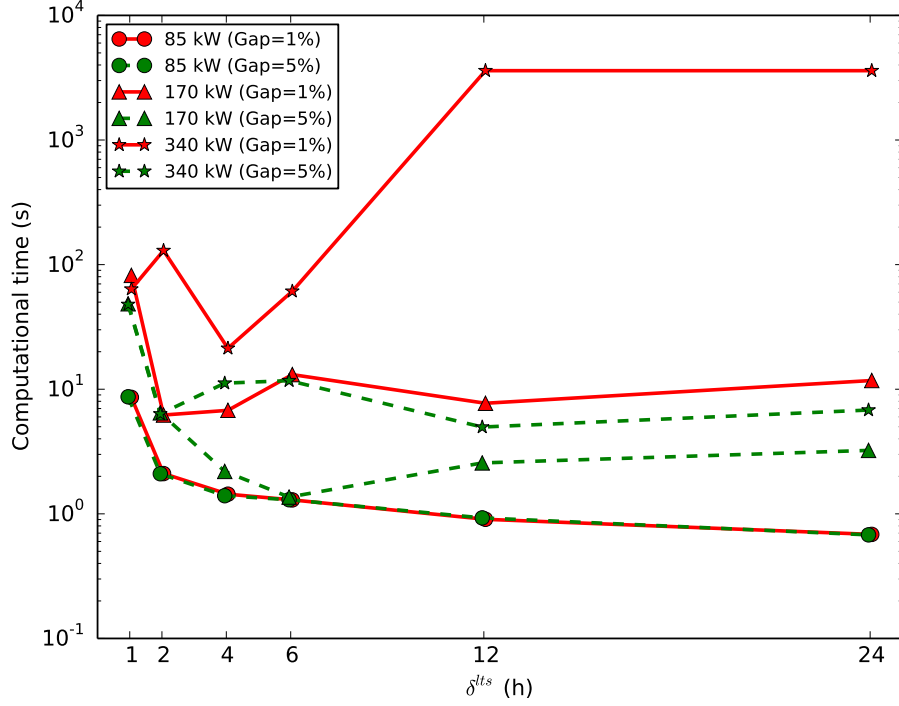
16

Figure 8: Computational time for optimisation run with different LTS charge/discharge power (kW) and MIP gap (%).

The STS size was selected to be 0.5 and 1.5 times of the original. All cases show similar trend of steep decrease in computational time as δ^{lts} goes from 1 to 2 h. The computational time has the tendency to increase again when δ^{lts} is larger than 4 and 6 h for 1% and 5% gap, respectively. In general, the STS size does not have a strong influence over the optimal LTS time grid size.

4.4. Optimisation with currently implemented control rules

One of the aims of performing the operational optimisation is to find the optimal operational profile of equipment in the system. Although it can be seen as too ideal for real application, the resulting profile can assist the engineers in designing the operational control of the system. It can also act as a benchmark to evaluate the real control options.

In order to evaluate the currently implemented control rules of the DLSC, an optimisation run with additional constraints describing the rules (Eq.22-23) was performed. In this optimisation run, the operational behaviour of LTS was only optimised during the summer period (May-Aug), while it was controlled by the implemented heuristic rules during the winter period (Sep-Apr).

The resulting LTS profiles of the reference and heuristic case are shown in Fig. 9. It is interesting to note that during most of the winter period (Sep-Mar),
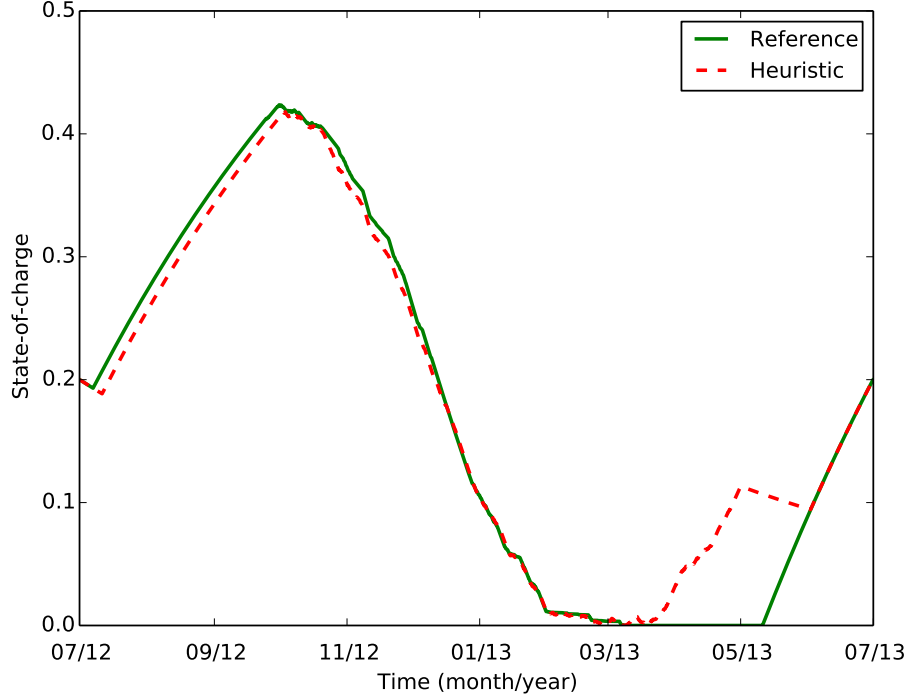
Figure 9: LTS state-of-charge profile for the optimised and heuristic case.

the heuristic model produced a very similar profile as the reference one although the LTS is controlled by the heuristic rules in this period. However, unlike the reference case, the LTS in the heuristic model starts charging immediately after March. This does not occur until after May in the reference case since it only needs to start charging at this time in order to fulfil the storage cyclic constraint. Furthermore, it can be seen that starting from May, the heuristic profile starts to follow the reference profile since from this point, the LTS is again optimised by the solver and not controlled by the heuristic rules.

Results of the reference optimised model, the heuristic model and field measurement are summarised in Table 4. The heuristic model was run to approximately 7% optimality gap due to resource constraints. It can be seen that the heuristic model produces results which are closer to the measurement than the optimised one. As expected, the objective value of the heuristic model is worse than the optimised model due to the assumed LTS charge/discharge rules during the winter period. The charging of LTS between March and May which occurs in the heuristic LTS profile (Fig. 9) is also reflected by the higher electricity consumption relative to the optimised model.

The relatively low value of the objective function in comparison to the size of the system is because only the natural gas for the boiler and the STS-LTS pump electricity consumption were included in the operational cost calculation.

18

Additionally, the gas and electricity price were the average price over the time horizon. In order to justify the overall size of the system, other contributing factors that can be considered include the pumping costs for all installed pumps, the heat losses in the system, and time-dependent price of gas and electricity. Furthermore, it should be noted that because of model assumption limitations and inherent complexity in the real control rules, comparison between models and measurement shown in Table 4 should be seen more on a qualitative level.

4.5. Multi-year optimisation

All optimisation runs in the previous sections were performed on a one year time horizon, with the assumed storage cyclic constraint. In order to evaluate the benefits of the multiple time grids approach in optimisation with longer time horizon, a multi-year optimisation run of the DLSC was performed. The resulting LTS operational profile of the multi-year SU optimisation is illustrated in Fig. 10. Similar to the annual optimisation result, the LTS is charging over the summer and discharging until depletion in the winter, with a rest period afterwards before it starts charging again. It is also interesting to note that the LTS state-of-charge never goes beyond 50% during the whole time horizon. This can be attributed to the overestimation of the LTS maximum capacity due to the implementation of the capacity model.

Table 5 compares the performance of SU and MU in the multi-year optimisation run. The MU was run with $\delta^{lts} = 6h$, which corresponds to the lowest computational time for the case study (see Fig. 7(a)) It has significantly faster computational time than the reference case, while maintaining a good agreement in objective value. The multi-year optimisation run exemplifies the main benefit of using multiple time grids method in the operational optimisation.

5. Conclusions

This study evaluates the benefits and trade-offs of using the multiple time grids method in the optimisation of an energy system which has thermal energy storage equipment with different temporal characteristics. It has been shown through a case study that the multiple time grids method can reduce the computational cost of energy system optimisation without significantly decreasing the results accuracy.

The case study was modelled as a mixed-integer linear programming problem and implemented with different time grids, i.e. single-uniform, multiple-uniform, and multiple-non-uniform. Although based on a specific case study, the key points shown in this paper are quite general in order to be considered when using multiple time grids in energy systems optimisation.

In the single-uniform case, the error in optimisation results grows as the time step increases. This will influence not only the operational optimisation, but also the design optimisation where equipment sizing is performed. Therefore, despite the significant reduction in computational time, increasing the step size in the single-uniform case is not recommended.
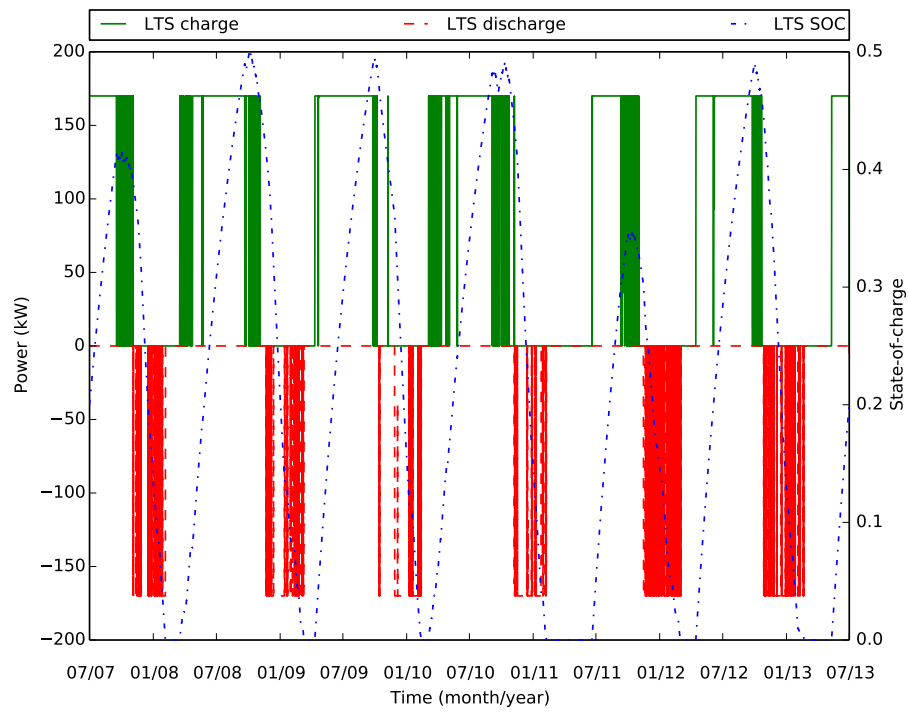
19

Figure 10: LTS operational profiles for multiple years optimisation (2007-2013).

In the multiple-uniform case, the computational time reduces significantly as the LTS time step size is increased from 1 h to 4-6 h, depending on the optimality gap. However, beyond this step size, the computational time has an increasing trend. Thus, increasing the time grid size of LTS does not guarantee an improvement in computational time. Unlike in the single-uniform case, the objective value does not suffer significantly when a larger LTS time step size is used. For the evaluated case study, the most significant computational time improvement occur in increasing the LTS time grid size from 1 to 2 h, with further improvement for larger grid size up to 6 h for the case with 5% MIP gap.

The LTS characteristics have significant influence over the benefits of using a larger time step size. For the case study, the benefit of using time step sizes larger than 4 h diminishes as the LTS thermal power increases. This should be taken into account if the multiple time grids method is to be used in design optimisation as different LTS characteristics may be considered in the optimisation. Moreover, it has been shown that the benefits of using multiple time grids becomes more apparent as a longer time horizon is considered.

In addition to the advantages of using the multiple time grids method, a careful selection of the time grids is necessary in order to avoid the unwanted computational time increase from using this method. On this aspect, one possible future research work is developing a systematic algorithm to generate the time grids which considers characteristics of different equipment (generation and storage) and demands (electricity, gas and heat).

It is also foreseen that the positive impacts of the multiple time grids method will be more significant on the design and synthesis-level of energy system optimisation. Further research work is needed in order to quantify the magnitude of these impacts. Moreover, the accuracy limit of the proposed method could be identified, for example, by comparing the objective function value with the results of a dynamic simulation, which uses the results of the operational optimisation as inputs.

Acknowledgements

Appendix A. Supplementary information

Supplementary information is available at `http://dx.doi.org/10.7488/ds/1516`.

References

[1] P. E. Dodds, S. D. Garvey, The role of energy storage in low-carbon energy systems, Storing Energy: with Special Reference to Renewable Energy Sources (2016) 1.

[2] W. A. Braff, J. M. Mueller, J. E. Trancik, Value of storage technologies for wind and solar energy, Nature Climate Change (June). doi:10.1038/nclimate3045.

[3] J. Kiviluoma, P. Meibom, Influence of wind power, plug-in electric vehicles, and heat storages on power system investments, Energy 35 (3) (2010) 1244–1255. doi:10.1016/j.energy.2009.11.004.
URL http://dx.doi.org/10.1016/j.energy.2009.11.004

[4] K. Hedegaard, O. Balyk, Energy system investment model incorporating heat pumps with thermal storage in buildings and buffer tanks, Energy 63 (2013) 356–365. doi:10.1016/j.energy.2013.09.061.
URL http://linkinghub.elsevier.com/retrieve/pii/S036054421300827X

[5] A. Ashouri, S. S. Fux, M. J. Benz, L. Guzzella, Optimal design and operation of building services using mixed-integer linear programming techniques, Energy 59 (2013) 365–376. doi:10.1016/j.energy.2013.06.053.
URL http://linkinghub.elsevier.com/retrieve/pii/S0360544213005525

[6] C. Wouters, E. S. Fraga, A. M. James, An energy integrated, multi-microgrid, MILP (mixed-integer linear programming) approach for residential distributed energy system planning â€“ A South Australian case-study, Energy 85 (2015) 30–44. doi:10.1016/j.energy.2015.03.051.
URL http://linkinghub.elsevier.com/retrieve/pii/S036054421500345X

[7] A. Rieder, A. Christidis, G. Tsatsaronis, Multi criteria dynamic design optimization of a small scale distributed energy system, Energy 74 (2014) 230–239. doi:10.1016/j.energy.2014.06.007.
URL http://dx.doi.org/10.1016/j.energy.2014.06.007

[8] M. Jennings, D. Fisk, N. Shah, Modelling and optimization of retrofitting residential energy systems at the urban scale, Energy 64 (2014) 220–233. doi:10.1016/j.energy.2013.10.076.
URL http://linkinghub.elsevier.com/retrieve/pii/S0360544213009432

[9] P. Voll, Automated optimization-based synthesis of distributed energy supply systems, Ph.D. thesis, RWTH Aachen (2013).

[10] C. Verhelst, F. Logist, J. Van Impe, L. Helsen, Study of the optimal control problem formulation for modulating air-to-water heat pumps connected to a residential floor heating system, Energy and Buildings 45 (2012) 43–53. doi:10.1016/j.enbuild.2011.10.015.
URL http://linkinghub.elsevier.com/retrieve/pii/S0378778811004592

[11] C. Milan, M. Stadler, G. Cardoso, S. Mashayekh, Modeling of non-linear CHP efficiency curves in distributed energy systems, Applied Energy 148 (2015) 334–347. doi:10.1016/j.apenergy.2015.03.053.
URL http://linkinghub.elsevier.com/retrieve/pii/S0306261915003372

[12] T. Schütz, R. Streblow, D. Müller, A comparison of thermal energy storage models for building energy system optimization, Energy and Buildings 93 (2015) 23–31. doi:10.1016/j.enbuild.2015.02.031.
URL http://linkinghub.elsevier.com/retrieve/pii/S037877881500136X

[13] T.-M. Tveit, T. Savola, A. Gebremedhin, C.-J. Fogelholm, Multi-period MINLP model for optimising operation and structural changes to CHP plants in district heating networks with long-term thermal storage, Energy Conversion and Management 50 (3) (2009) 639–647. doi:10.1016/j.enconman.2008.10.010.
URL http://linkinghub.elsevier.com/retrieve/pii/S0196890408004159

[14] F. M. Rad, A. S. Fung, M. a. Rosen, An integrated model for designing a solar community heating system with borehole thermal storage, Energy for Sustainable Development 36 (2017) 6–15. doi:10.1016/j.esd.2016.10.003.
URL http://dx.doi.org/10.1016/j.esd.2016.10.003

[15] L. Yang, E. Entchev, A. Rosato, S. Sibilio, Smart Thermal Grid with Integration of Distributed and Centralized Solar Energy Systems, Energy 122 (2017) 471–481. doi:10.1016/j.energy.2017.01.114.
URL http://dx.doi.org/10.1016/j.energy.2017.01.114

[16] C. A. Floudas, X. Lin, Continuous-time versus discrete-time approaches for scheduling of chemical processes: a review, Computers & Chemical Engineering 28 (11) (2004) 2109–2129. doi:10.1016/j.compchemeng.2004.05.002.
URL http://linkinghub.elsevier.com/retrieve/pii/S0098135404001401

[17] S. Velez, C. T. Maravelias, Multiple and nonuniform time grids in discrete-time MIP models for chemical production scheduling, Computers and Chemical Engineering 53 (2013) 70–85. doi:10.1016/j.compchemeng.2013.01.014.
URL http://dx.doi.org/10.1016/j.compchemeng.2013.01.014

[18] S. Velez, C. T. Maravelias, Theoretical framework for formulating MIP scheduling models with multiple and non-uniform discrete-time grids, Computers & Chemical Engineering 72 (2014) 233–254. doi:10.1016/j.compchemeng.2014.03.003.
URL http://linkinghub.elsevier.com/retrieve/pii/S0098135414000702

[19] J. R. Winkelman, J. H. Chow, J. J. Allemong, P. V. Kokotovic, Multi-Time-Scale Analysis of a Power System, Automatica 16 (1980) 35–43.

[20] A. Kargarian, G. Hug, J. Mohammadi, A Multi-Time Scale Co-Optimization Method for Sizing of Energy Storage and Fast-Ramping Generation, IEEE Transactions on Sustainable Energy 7 (4) (2016) 1351–1361.

[21] K. G. Boroojeni, M. H. Amini, S. Bahrami, S. S. Iyengar, A. I. Sarwat, O. Karabasoglu, A novel multi-time-scale modeling for electric power demand forecasting : From short-term to medium-term horizon, Electric Power Systems Research 142 (2017) 58–73. doi:10.1016/j.epsr.2016.08.031.
URL http://dx.doi.org/10.1016/j.epsr.2016.08.031

[22] G. Mavrotas, K. Florios, D. Vlachou, Energy planning of a hospital using Mathematical Programming and Monte Carlo simulation for dealing with uncertainty in the economic parameters, Energy Conversion and Management 51 (4) (2010) 722–731. doi:10.1016/j.enconman.2009.10.029.
URL http://linkinghub.elsevier.com/retrieve/pii/S0196890409004373

[23] J. Ortiga, J. Bruno, a. Coronas, Selection of typical days for the characterisation of energy demand in cogeneration and trigeneration optimisation models for buildings, Energy Conversion and Management 52 (4) (2011) 1934–1942. doi:10.1016/j.enconman.2010.11.022.
URL http://linkinghub.elsevier.com/retrieve/pii/S0196890410005315

[24] F. Domínguez-Muñoz, J. M. Cejudo-López, A. Carrillo-Andrés, M. Gallardo-Salazar, Selection of typical demand days for CHP optimization, Energy and Buildings 43 (11) (2011) 3036–3043. doi:10.1016/j.enbuild.2011.07.024.
URL http://linkinghub.elsevier.com/retrieve/pii/S037877881100329X

[25] S. Fazlollahi, S. L. Bungener, P. Mandel, G. Becker, F. Maréchal, Multi-Objectives, Multi-Period Optimization of district energy systems: I-Selection of typical operating periods, Computers & Chemical Engineering 65 (2014) 54–66. doi:10.1016/j.compchemeng.2014.03.005.
URL http://linkinghub.elsevier.com/retrieve/pii/S0098135414000751

[26] S. Fazlollahi, G. Becker, F. Maréchal, Multi-objectives, multi-period optimization of district energy systems: IIâ€"Daily thermal storage, Computers & Chemical Engineering 71 (2014) 648–662. doi:10.1016/j.compchemeng.2013.10.016.
URL http://linkinghub.elsevier.com/retrieve/pii/S0098135413003384

24

[27] J. Söderman, F. Pettersson, Structural and operational optimisation of distributed energy systems, Applied Thermal Engineering 26 (13) (2006) 1400–1408. doi:10.1016/j.applthermaleng.2005.05.034.
URL http://linkinghub.elsevier.com/retrieve/pii/S1359431105002164

[28] S. Samsatli, N. J. Samsatli, A general spatio-temporal model of energy systems with a detailed account of transport and storage, Computers & Chemical Engineering 80 (2015) 155–176. doi:10.1016/j.compchemeng.2015.05.019.
URL http://linkinghub.elsevier.com/retrieve/pii/S0098135415002008

[29] J. M. F. Rager, Urban Energy System Design from the Heat Perspective using mathematical programming including thermal storage, Ph.D. thesis, Ecole Polytechnique Federale de Lausanne (2015).

[30] M. G. Ierapetritou, C. A. Floudas, Effective Continuous-Time Formulation for Short-Term Scheduling. 1. Multipurpose Batch Processes, Industrial & Engineering Chemistry Research 37 (11) (1998) 4341–4359. doi:10.1021/ie970927g.
URL http://pubs.acs.org/doi/abs/10.1021/ie970927g

[31] M. G. Ierapetritou, C. A. Floudas, Effective continuous-time formulation for short-term scheduling. Part 2. Continuous and semicontinuous processes, Industrial & Engineering Chemistry Research 37 (11) (1998) 4360–4374. doi:10.1021/ie9709289.

[32] P. M. Castro, I. E. Grossmann, New continuous-time MILP model for the short-term scheduling of multistage batch plants, Industrial and Engineering Chemistry Research 44 (24) (2005) 9175–9190. doi:10.1021/ie050730l.

[33] D. Bauer, R. Marx, J. Nuß bicker Lux, F. Ochs, W. Heidemann, H. Müller-Steinhagen, German central solar heating plants with seasonal heat storage, Solar Energy 84 (4) (2010) 612–623. doi:10.1016/j.solener.2009.05.013.
URL http://linkinghub.elsevier.com/retrieve/pii/S0038092X09001224

[34] B. Sibbitt, D. McClenahan, R. Djebbar, J. Thornton, B. Wong, J. Carriere, J. Kokko, The performance of a high solar fraction seasonal storage district heating system - Five years of operation, Energy Procedia 30 (2012) 856–865. doi:10.1016/j.egypro.2012.11.097.
URL http://dx.doi.org/10.1016/j.egypro.2012.11.097

[35] H. J. Quintana, M. Kummert, Optimized control strategies for solar district heating systems, Journal of Building Performance Simulation (January 2015) (2014) 1–18. doi:10.1080/19401493.2013.876448.
URL http://www.tandfonline.com/doi/abs/10.1080/19401493.2013.876448

[36] M. Shaarawy, M. Lightstone, Numerical Analysis of Thermal Stratification in Large Horizontal Thermal Energy Storage Tanks, Journal of Solar Energy Engineering 138 (April). doi:10.1115/1.4032451.

[37] P. Kandiah, M. F. Lightstone, Modelling of the thermal performance of a borehole field containing a large buried tank, Geothermics 60 (2016) 94–104. doi:10.1016/j.geothermics.2015.12.001.
URL http://dx.doi.org/10.1016/j.geothermics.2015.12.001

[38] C. Flynn, K. Sirén, Influence of location and design on the performance of a solar district heating system equipped with borehole seasonal storage, Renewable Energy 81 (2015) 377–388. doi:10.1016/j.renene.2015.03.036.
URL http://linkinghub.elsevier.com/retrieve/pii/S0960148115002189

[39] Leidos Canada, Drake Landing Solar Community, Annual Performance Monitoring Report for 2012-2013, Leidos Canada (2014).

[40] H. Quintana, A Practical Approach to Model Predictive Control (MPC)for Solar Communities, Ph.D. thesis, École Polytechnique de Montréal (2013).
URL http://publications.polymtl.ca/1146/

[41] M. Shaarawy, Numerical Analysis of Thermal Stratification in Large Horizontal Thermal Energy Storage Tanks, Master of applied science thesis, McMaster University (2014).

[42] T. P. McDowell, J. W. Thornton, Simulation and model calibration of a large-scale solar seasonal storage system, Third national conference of IBPSA-USA (2008) 174–181.

[43] Alberta Government, Utilities consumer advocate - historic rates (2016).
URL http://http://ucahelps.alberta.ca/historic-rates.aspx

[44] R. Renaldi, a. Kiprakis, D. Friedrich, An optimisation framework for thermal energy storage integration in a residential heat pump heating system, Applied Energydoi:10.1016/j.apenergy.2016.02.067.
URL http://linkinghub.elsevier.com/retrieve/pii/S0306261916302045

[45] Government of Canada, Historical climate data (2016).
URL http://climate.weather.gc.ca/

[46] National Resources Canada, Drake landing satellite solar resource data (2015).
URL ftp://ftp.nrcan.gc.ca/energy/SOLAR/DrakeLanding_SatteliteSolarResourceData/

[47] W. E. Hart, C. Laird, J.-P. Watson, D. L. Woodruff, Pyomo–optimization modeling in python, Vol. 67, Springer Science & Business Media, 2012.

[48] IBM, IBM CPLEX Optimizer (2015).
URL `http://www-01.ibm.com/software/commerce/optimization/cplex-optimizer/index.html`

[49] A. Hawkes, M. Leach, Impacts of temporal precision in optimisation modelling of micro-Combined Heat and Power, Energy 30 (10) (2005) 1759–1779. doi:10.1016/j.energy.2004.11.012.
URL `http://linkinghub.elsevier.com/retrieve/pii/S036054420400475X`

[50] T. Wakui, R. Yokoyama, Impact analysis of sampling time interval and battery installation onÂ optimal operational planning of residential cogeneration systems without electric power export, Energydoi:10.1016/j.energy.2014.12.002.
URL `http://linkinghub.elsevier.com/retrieve/pii/S0360544214013541`

Table 2: Parameter values

	Parameter	Unit	Value	Reference
SCO	η^{sco}		0.5	Assumption
	A^{sco}	m^2	2293	[34]
STS	V^{sts}	m^3	240	[34]
	ρ_w	kg/m^3	1000	
	c_w	kJ/kg·K	4.2	
	ΔT^{sts}	K	50	[41]
	ϕ_{sts}	%	0.02	Assumption
	Q_{max}^{sts}	MWh	14	Eq. (3)
	$\dot{Q}_{ch,max}^{sts}$	kW	2940	Charging flow rate = 14 l/s; Case 2 in [41]
	$\dot{Q}_{dch,max}^{sts}$	kW	1260	Discharging flow rate = 6 l/s; Case 1 in [41]
	$SOC_{t=0}^{sts}$	-	1.0	Assumption
LTS	V^{lts}	m^3	33700	[34]
	$\rho_s \cdot c_s$	kJ/m^3·K	3203	[42]
	k_s	W/m·K	1.373	[42]
	ΔT^{lts}	K	30	[39]
	ϕ_{lts}	%	0.024	Assumption
	Q_{max}^{lts}	MWh	900	Eq. (10)
	$\dot{Q}_{ch,max}^{lts}$	kW	170	Avg. charging flow rate = 2.7 l/s [39]
	$\dot{Q}_{dch,max}^{lts}$	kW	170	Avg. discharging flow rate = 2.7 l/s [39]
	$SOC_{t=0}^{lts}$	-	0.2	Assumption
	P_{pump}	kW	0.5	Assumption
BOI	η^{boi}		0.9	Assumption
	$\dot{Q}_{max}^{boi}$	kW	1000	Assumption
Natural gas	C_{gas}	\$/kWh	0.011	Average rate, July 2012 - June 2013 [43].
Electricity	C_{el}	\$/kWh	0.0866	Average rate, July 2012 - June 2013 [43].

28

Table 3: Computational results for the reference case

Time grids	SU
Time step size (h)	1
Binary variables	17522
Total variables	96372
Average computational time (s)	82.2
Relative gap	0.01
Objective value ($)	264
Solar energy collected (GJ)	5630
Solar energy to STS (GJ)	3677
STS charge (GJ)	4587
STS discharge (GJ)	4564
LTS charge (GJ)	2089
LTS discharge (GJ)	909
Solar energy to district (GJ)	2474
Gas consumption (GJ)	15

Table 4: Results of the optimised model, heuristic model and measurement.

	Optimised model	Heuristic model	Measurement [39]
Solar energy collected (GJ)	5630.4	5630.4	4328.3
Solar energy to STS (GJ)	3676.7	3700.8	4590.3[*]
LTS charge (GJ)	2089.4	2360.8	2566.2
LTS discharge (GJ)	908.9	1132.4	1306.8
Solar energy to district (GJ)	2473.4	2442.2	2434[*]
Gas consumption (GJ)	15.5	47.0	42.4
Electricity (GJ)	9	13.7	-
Objective value ($)	264.8	475	-

*Measurements error due to sensors imperfect calibration [39].

Table 5: Details of single uniform and multiple uniform optimisation of the multiple years case.

	SU	MU
Binary variable	105218	17538
Total variable	578700	359500
Computational time (s)	1985	121 (-94%)
MIP gap	5%	5%
Objective value ($)	4493	4534 (+0.9%)